Table I. Ground- and Excited-State Resonance Raman Frequencies

ground state			excited state		
$Ru(bpy)_3^{2+}$	Ru-$(bpy\text{-}d_2)_3^{2+}$	Δd	$Ru(bpy)_3^{2+}$	Ru-$(bpy\text{-}d_2)_3^{2+}$	Δd
1608	1591	17	1608	1590	18
			1550	1535	15
1563	1553	10			
1493	1469	24	1500	1478	22
			1429	1427	2
1320	1298	22	1324	*b*	~20
			1288	1271	17
1276	1253				
			1215	1186	
1266	1223		1103	1110	
1175	1129		1025	1071	
1043	1084			1022	
1030	1016		1015	1004	11
			744	737	7
669	660	9			

[a] Δd is a given for correlated modes only. [b] Appears as an unresolved shoulder.

The excited-state spectra were obtained with an excitation line nearly coincident with the π–π^* excited-state absorption band at ~350 nm, which presumably corresponds to a transition of a coordinated ligand anion radical. As Woodruff and Dallinger and co-workers[2] have pointed out, the localized model is also consistent with observation of bands assignable to the neutral ligand through resonance with the π–π^* transition at ~280 nm. The data presented in Table I, including the observed deuterium shifts, are entirely consistent with expected behavior.

The most noteworthy feature of the excited-state spectrum is the appearance of a band at 1429 cm^{-1}, which exhibits an insignificant deuterium shift. No ground-state bands observed in this region under visible (MLCT) excitation exhibit similar behavior. It is likely that the 1429-cm^{-1} band corresponds to the very weak ground-state band at 1450 cm^{-1}, which is only observed with excitation at ~350 nm (continuous wave).[2,3,9] Evidently this band is not enhanced under MLCT excitation. We have attempted to observe a corresponding band in the spectrum of the deuterated analogue using 363.8-nm (continuous wave) Ar^+ laser excitation but were unable to confirm its appearance, possibly because of overlap with the 1469-cm^{-1} band. The 1608-cm^{-1} ground-state band corresponds to the 1608- (neutral ligand) and 1550-cm^{-1} (radical anion) bands in the excited state; all bands exhibited comparable deuterium shifts. Similarly, the 1320-cm^{-1} ground-state band occurs at 1324 cm^{-1} (neutral ligand) and 1288 cm^{-1} (radical anion) in the excited state again exhibiting deuterium shifts of similar magnitude. The 1493- and 1563-cm^{-1} ground-state bands[2,3,9] as well as the first overtone of the 744-cm^{-1} band probably all contribute to the excited-state feature at ~1500 cm^{-1}, although we were not able to resolve the components in this region. No band was observed that could be correlated with a radical anion band corresponding to the 1493-cm^{-1} ground-state band. Apparently this band exhibits an insignificant shift in the radical anion or is not enhanced in the excited state (π–π^* excitation). Several bands below 1300 cm^{-1} in the ground- and excited-state spectra shift substantially upon deuteration but are too weak to correlate reliably at this time. However, future work involving deuteration at other sites combined with excitation profiles of the excited state will help to establish correlations of these and higher frequency bands. The excited-state band observed at 1735 cm^{-1} (1004 + 737 cm^{-1}) in the spectrum of the deuterated analogue is consistent with the assignment of the 1753-cm^{-1} (1015 + 744 cm^{-1}) combination band in the parent compound.[3]

In summary, consideration of deuterium shifts for ground- and excited-state bands provides a more reliable estimate of excited-state frequency shifts. The observations presented here indicate that ground- and excited-state bands may not be correlated on a strict one-to-one basis and that some ground-state bands that correspond to "radical anion" (π–π^* enhanced) bands in the excited state are not enhanced under visible (MLCT) excitation. Nevertheless, substantial shifts are associated with formation of the excited state. These are, in fact, comparable to shifts observed for the well-studied biphenyl[7] and bipyridyl[8] anion radicals and lend further support to the previous interpretations[2,3,9] of rR data as evidence for the localized excited state model.

Acknowledgment. We express our sincere appreciation to Professor Thomas Spiro of Princeton University for use of equipment and facilities and to Professors F. J. Holler and L. M. Tolbert of the University of Kentucky for technical assistance and helpful discussions. This work was supported by the Graduate School of the University of Kentucky. S.M. thanks the Ashland Oil Corp. for a summer fellowship.

(9) Smothers, W. K.; Wrighton, M. S. *J. Am. Chem. Soc.* **1983**, *105*, 1067–1069.

Structure and Bonding of the First η^2-Coordinated P_4 Ligand: Molecular Structure of *trans*-$[Rh(P_4)(PPh_3)_2Cl]\cdot 2CH_2Cl_2$ at 185 K

W. Edward Lindsell and Kevin J. McCullough

Department of Chemistry, Heriot-Watt University Edinburgh EH14 4AS, Scotland, U.K.

Alan J. Welch*

Department of Chemistry, University of Edinburgh Edinburgh EH9 3JJ, Scotland, U.K.

Received February 24, 1983

Although the complex $Rh(P_4)(PPh_3)_2Cl$ (**1**)[1,2] and related derivatives of Rh[1,2] and Ir[2] were synthesized several years ago, the precise nature of the novel M–P_4 interaction was not established. In the more recently characterized complexes $M[N(CH_2CH_2PPh_2)_3]P_4$ (**2**, M = Ni; **3**, M = Pd)[3-5] the P_4 tetrahedron is η^1-coordinated to the metal. For complex **1**, however, the alternative η^2- or η^3-coordination modes are also feasible. Indeed, a very recent NMR study[6] of **1** suggested η^2-coordination for the P_4 unit.

It was clearly of considerable importance to characterize **1** by X-ray diffraction, to corroborate the conclusions of the NMR experiment and also to furnish accurate structural parameters for the coordinated P_4 moiety (errors in P–P lengths in the structural study of **2** being rather large). Progress had been initially frustrated by decomposition of solutions and crystals of **1** at temperatures >260 K. Recrystallization from dichloromethane at 195 K has now, however, afforded suitable crystals as a solvate ($Rh:CH_2Cl_2$ = 1:2), which on rapid transference to a diffractometer equipped with a low-temperature attachment enabled an accurate structural study to be undertaken.[7]

(1) Ginsberg, A. P.; Lindsell, W. E. *J. Am. Chem. Soc.* **1971**, *93*, 2082–2084.

(2) Ginsberg, A. P.; Lindsell, W. E.; Silverthorn, W. E. *Trans. N.Y. Acad. Sci.* **1971**, *33*, 303–312.

(3) Dapporto, P.; Midollini, S.; Sacconi, L. *Angew. Chem., Int. Ed. Engl.* **1979**, *18*, 469.

(4) Dapporto, P.; Sacconi, L.; Stoppioni, P.; Zanobini, F. *Inorg. Chem.* **1981**, *20*, 3834–3839.

(5) Di Vaira, M.; Sacconi, L. *Angew Chem., Int. Ed. Engl.* **1982**, *21*, 330–342.

(6) Lindsell, W. E. *J. Chem. Soc., Chem. Commun.* **1982**, 1422–1424.

0002-7863/83/1505-4487$01.50/0

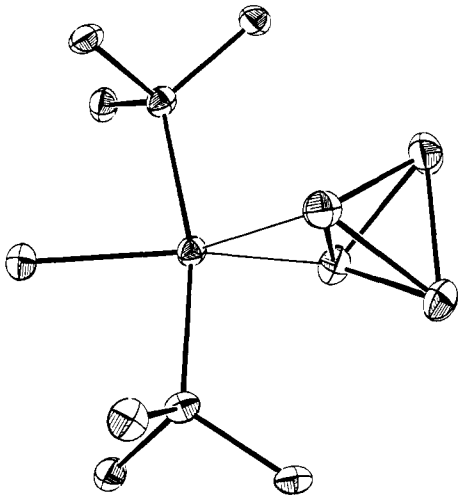

Figure 1. Perspective view (ORTEPII, 50% probability thermal ellipsoids) of complex **1** with most of the phenyl groups omitted for clarity. Important molecular parameters: Rh(1)–Cl(1), 2.4095 (14); Rh(1)–P(1), 2.3340 (14); Rh(1)–P(2), 2.3312 (14); Rh(1)–P(3), 2.3016 (16); Rh(1)–P(4), 2.2849 (16); P(3)–P(4), 2.4616 (22) Å; P(1)–Rh(1)–Cl(1), 82.65 (5); P(2)–Rh(1)–Cl(1), 83.56 (5); P(3)–Rh(1)–P(4), 64.92 (5)°.

The crystal structure consists of well-separated molecules of solvent and the complex **1**, a perspective view of which is given, together with important molecular parameters, in Figure 1. The crystallographic analysis confirms the essential stereochemistry determined by the NMR study[6] of **1**, viz., the P_4 function is η^2-coordinated with the metal-bonded P–P edge perpendicular to the ligand plane, the local geometry of which is a distorted square plane (the triphenylphosphine groups bend away from the P_4 ligand, cf. $Rh(PPh_3)_3Cl$ (**4**) and *trans*-$Rh(PPh_3)_2(C_2F_4)Cl$ (**5**)[10]).

The Rh–P(3,4) distances in **1** are 2.3016 (16) and 2.2849 (16) Å, respectively, and the most important deformation of the P_4 molecule (from a regular tetrahedral geometry of dimension 2.21 Å[11]) is a lengthening (ca. 0.25 Å) of the metal-bonded edge upon coordination. Although the opposite edge, P(5)–P(6), is the shortest in the coordinated ligand (by ca. 0.02 Å), we do not attach great significance to this result, as (i) its difference in length from the four adjacent edges is comparable with their internal variation and (ii) shortening of P(5)–P(6) is not reproduced theoretically (vide infra).

A strong structural analogy between η^2-coordinated P_4 and coordinated alkenes arises since η^2-alkene ligands also bond perpendicularly in square-planar ML_3(alkene) complexes,[12] with concomitant C=C bond lengthening. To explore this analogy further, we have carried out EHMO calculations on **1**, with parameters specified in ref 13.

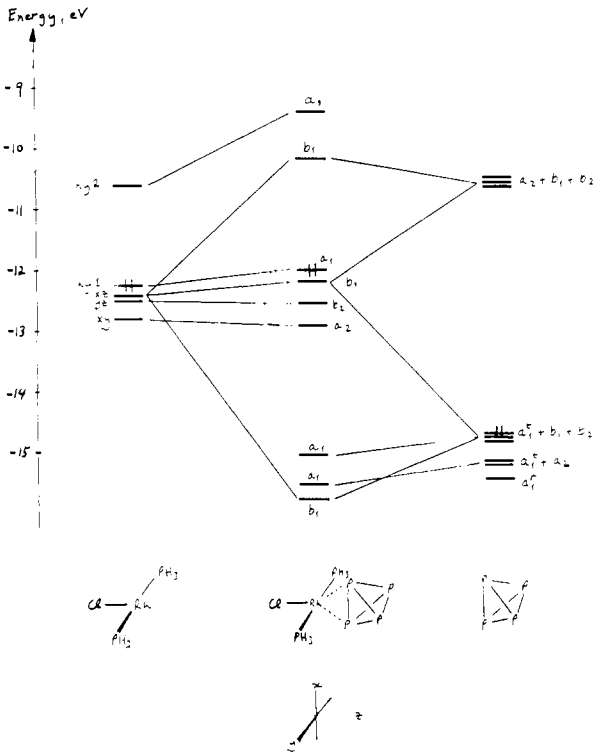

Figure 2. Interaction diagram for $[Rh(\eta^2\text{-}\perp\text{-}P_4)(PH_3)_2Cl]$. The metal orbitals hyl and hy2 are hybrids localized along the *z* and *x* axes respectively.

Figure 2 shows the interaction diagram for $Rh(PH_3)_2Cl$ and P_4 fragments to yield a complex with η^2-$\perp$ stereochemistry, and for consistency the MO's of P_4 are described in only C_{2v} symmetry. The frontier orbitals of the metal fragment are well-known;[12,16,17] in P_4 the six highest occupied MO's are largely s–p hybrids, and the lowest unoccupied MO's are p–d hybrids. In Figure 2, a_1 MO's are subdivided as a_1^t if they lie tangential to the P_4 polyhedron and a_1^r if they radiate from it; examples of these are shown in I (a_1^t at −15.22 eV) and II (a_1^r at −15.45 eV).

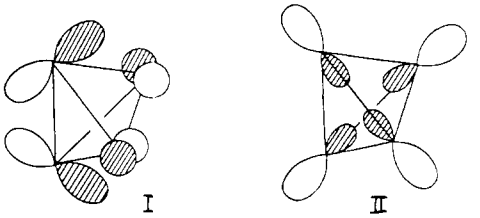

The alkene–transition metal bond is classically described by the complementary interactions of alkene π and metal acceptor orbitals (σ) and alkene π^* and metal donor orbitals (π). For η^2-P_4 it is clearly the filled a_1^t ligand orbitals that interact with the metal LUMO to provide the σ component of the bonding. Although the energy separation is substantial (ca. 4 eV vs. ca. 2.5 eV when P_4 is replaced by C_2H_4), the interaction is clearly stabilizing and apparently sufficiently strong to lengthen the *trans*-Rh–Cl bond

(7) Crystal data: $C_{36}H_{30}ClP_6Rh\cdot 2CH_2Cl_2$, amber platelets, triclinic, a = 11.853 (2) Å, b = 12.568 (8) Å, c = 14.505 (2) Å, α = 104.41 (4)°, β = 103.42 (13)°, γ = 84.22 (4)°, U = 2033.5 (19) Å^3, D_o = 1.58 g cm^{-3}, Z = 2, D_c = 1.562 g cm^{-3}, $F(000)$ = 986 electrons, μ(MoKα) = 9.8 cm^{-1}, space group $P\bar{1}$ from E statistics and successful refinement. A total of 7137 unique intensities, from a crystal of approximate dimensions 0.2 × 0.3 × 0.4 mm, was recorded (θ–2θ scans) at 185 ± 1 K to θ_{max} = 25° (graphite-monochromated MoKα X-radiation, λ = 0.71069 Å) on an Enraf-Nonius CAD4 diffractometer. Corrections for absorption were not applied. The structure was solved by Patterson (Rh) and difference Fourier techniques and refined by full-matrix least-squares (SHELX76[8]) to an R value of 0.0456, with a weighted index R_w ($=\sum w||F_o| - |F_c||/\sum w^{1/2}|F_o|$) of 0.0625 ($w^{-1} = \sigma^2(F_o) + 0.0034F_o^2$) for 5245 reflections with $F_o \geq 2\sigma(F_o)$. Except for the methylene carbon atoms, all non-hydrogen atoms were allowed anisotropic thermal motion. Phenyl groups were treated as rigid, planar hexagons (C–C = 1.395 Å), and all hydrogen atoms were set in idealized positions (C–H = 1.08 Å) with fixed thermal parameters.[9]

(8) Sheldrick, G. M. University of Cambridge, 1976.

(9) Full data will be published elsewhere.

(10) Hitchcock, P. B.; McPartlin, M.; Mason, R. *J. Chem. Soc., Chem. Commun.* **1969**, 1367–1368.

(11) Sutton, L. E., Ed. *Chem. Soc., Spec. Publ.* **1958**, *No. 11*.

(12) Albright, T. A.; Hoffmann, R.; Thibeault, J. C.; Thorn, D. L. *J. Am. Chem. Soc.* **1979**, *101*, 3801–3812 and references therein.

(13) EHMO calculations[14] on *trans*-$Rh(PH_3)_2Cl$ and *trans*-$Rh(P_4)(PH_3)_2Cl$ in strict C_{2v} symmetry with square-planar geometry and on P_4 in strict T_d symmetry. Distances (Å) used: Rh–PH_3, 2.33; Rh–P_4, 2.25; Rh–Cl, 2.41; P–H, 1.42; P–P, 2.21. Rh–P–H and H–P–H angles, 109.47°. The values for Rh H_{ii}'s and orbital exponents were taken from ref 15. For P and Cl, 3d orbitals were included with H_{ii} = −7.0 eV, Slater exponent = 1.4, and H_{ii} = −9.0 eV, Slater exponent = 2.033, respectively.

(14) Howell, J.; Rossi, A.; Wallace, D.; Haraki, K.; Hoffmann, R. *QPCE* **1977**, *10*, 344.

(15) Hoffman, D. M.; Hoffmann, R.; Fisel, C. R. *J. Am. Chem. Soc.* **1982**, *104*, 3858–3875. The lower set of values of their Table III were used.

(16) Eisenstein, O.; Hoffmann, R. *J. Am. Chem. Soc.* **1981**, *103*, 4308–4320.

(17) Hoffmann, R. *Angew Chem., Int. Ed. Engl.* **1982**, *21*, 711–724.

by ca. 0.035 Å relative to that in **4** and **5**.[10]

A fundamental difference is found to exist between the π components of metal-alkene and metal-(η^2-P_4) bonding, in that the former involves a 2e-2 MO system while for the latter a 4e-3 MO framework is produced (b_1 symmetry in Figure 2) involving both filled and unfilled ligand orbitals[18].

The perpendicular conformation on the η^2-bonded P_4 ligand is favored with respect to the parallel conformation by increased π bonding. EHMO calculations on perpendicular and parallel models of $[Rh(P_4)(PH_3)_2Cl]$ show that both types of Rh-P bond are weakened in the latter,[19] and yield a barrier to rigid rotation of the P_4 ligand, about the z axis, of ca. 5 eV.

Computed overlap populations for the η^2-$\perp$ model successfully reproduce the weakening of the P(3)-P(4) connectively that is inferred from its crystallographically observed lengthening. It is noteworthy that the opposite tetrahedral edge is not substantially altered upon formation of complex **1**, possibly suggesting that complexes with bridging di-(η^2)-P_4 ligands might be feasible. Furthermore, given the overall strength of the Rh-P_4 bonding, we can see no prima facie reason why other examples of η^2-coordinated P_4 should not be amenable to synthesis. Experiments designed to explore these possibilities are currently in hand.

Registry No. 1·$2CH_2Cl_2$, 85939-99-7.

Supplementary Material Available: Atom coordinates (Table 1), thermal parameters (Table 2), internuclear distances (Table 3), and interbond angles (Table 4) (4 pages). Ordering information is given on any current masthead page.

(18) The iridium analogue of **1**, with higher lying metal valence orbitals, presumably has a weaker M-P_4 σ bond and a π interaction more closely similar to that of an alkene complex.

(19) Overlap populations: $\perp$, Rh-P_4, 0.355; Rh-PH_3, 0.530; P-P, 0.689 (metal-bonded edge), 0.782 (opposite edge), 0.788 (other edges); $\parallel$, Rh-P_4, 0.129; Rh-PH_3, 0.350.

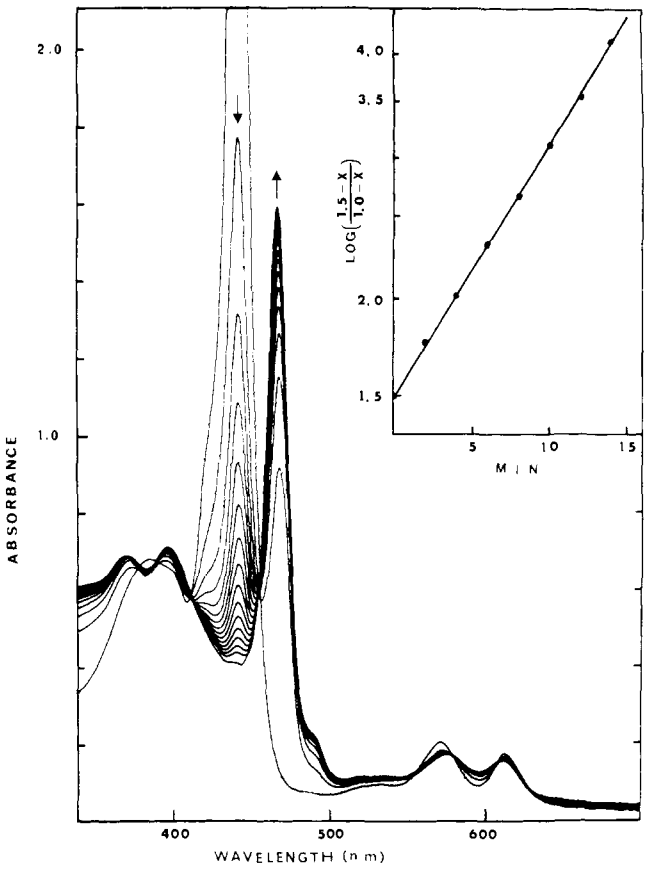

Figure 1. Visible spectral changes for the reaction of 1.5 equiv of *m*-chlorobenzoyl chloride with $TMPMn^{II}$-O_2^- (**1**) in acetonitrile at -20 °C. Inset: second-order plot of the time course of the decrease of **1**, $X = (A_0 - A_t)/(A_0 - A_\infty)$ at 445 nm, 1.3×10^{-5} M.

Oxygen Activation by Metalloporphyrins. Formation and Decomposition of an Acylperoxymanganese(III) Complex

John T. Groves,* Yoshihito Watanabe, and Thomas J. McMurry

Department of Chemistry, The University of Michigan Ann Arbor, Michigan 48109

Received February 8, 1983

The catalytic cycle of the monooxygenase cytochrome P-450 is considered to involve the binding and reduction of molecular oxygen at the heme center and ultimate formation of a reactive iron oxo complex that is responsible for the oxidation of the substrate.[1] While synthetic porphyrin complexes have been shown to bind oxygen[2] and to be oxidized to oxometalloporphyrin complexes capable of oxidizing even saturated hydrocarbons,[3] the conversion of a metalloporphyrin-dioxygen complex to a reactive oxo species is still without precedent in model systems.[4] In this paper we demonstrate (i) the acylation of an oxygenated manganese-porphyrin complex to form an acylperoxymanganese(III) complex, (ii) the independent preparation of this acylperoxy complex by the direct addition of peroxyacid salts, (iii) the decomposition of the acylperoxymanganese(III) complex to an oxomanganese(V) species, and (iv) oxygen atom transfer from this manganese oxo complex to olefins to regenerate the starting manganese(III) porphyrin.

Scheme I

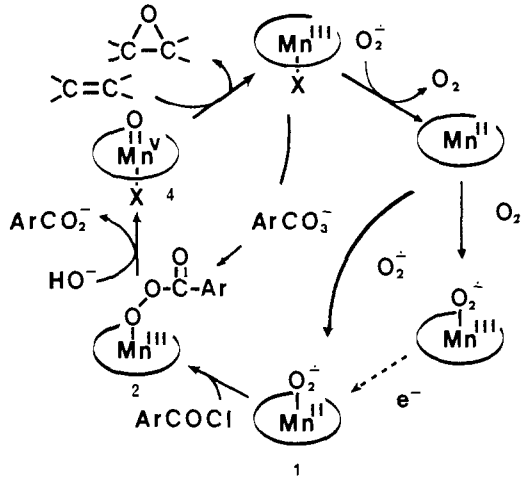

1

(1) (a) White, R. E.; Coon, M. J. *Ann. Rev. Biochem.* **1980**, *49*, 315-356. (b) Gunsalus, I. C.; Sligar, S. G. *Adv. Enzymol. Relat. Areas Mol. Biol.* **1978**, *47*, 1-44. (c) Omura, T. In "Cytochrome P-450"; Sato, R., Omura, T., Eds.; Kodansha Ltd.: Tokyo, 1978; pp 138-163.

(2) (a) Collman, J. P.; Gagne, R. R.; Reed, C. A.; Halbert, T. R.; Lang, G.; Robinson, W. T. *J. Am. Chem. Soc.* **1975**, *97*, 1427-1439. (b) Collman, J. P.; Brauman, J. I.; Collins, T. J.; Iverson, B.; Sessler, J. L. *Ibid.* **1981**, *103*, 2450-2452. (c) Hashimoto, T.; Dyer, R. L.; Crossley, M. J.; Baldwin, J. E.; Basolo, F. *Ibid.* **1982**, *104*, 2101-2109. (d) Traylor, T. G.; Mitchell, M. J.; Tsuchiya, S.; Campbell, D. H.; Stynes, D. V.; Koga, N. *Ibid.* **1981**, *103*, 5234-5236.

(3) (a) Groves, J. T.; Nemo, T. E.; Myers, R. S. *J. Am. Chem. Soc.* **1979**, *101*, 1032-103. (b) Chang, C. K.; Kuo, M.-J. *Ibid.* **1979**, *101*, 3413-341. (c) Groves, J. T.; Kruper, W. J., Jr.; Haushalter, R. C. *Ibid.* **1980**, *102*, 6375-6377. (d) Hill, C. L.; Schardt, B. C. *Ibid.* **1980**, *102*, 6374-6375. (e) Groves, J. T.; Haushalter, R. C.; Nakamura, M.; Nemo, T. E.; Evans, B. J. *Ibid.* **1981**, *103*, 2884-2886. (f) Smith, J. R. L.; Sleath, P. R. *J. Chem. Soc., Perkin Trans. 2* **1982**, 1009-1015.

(4) For two systems that potentially proceed in this way see: (a) Tabushi, I.; Yazaki, A. *J. Am. Chem. Soc.* **1981**, *103*, 7371-7373. (b) Kheukin, A. M.; Shteinman, A. A. *Kinet. Katal.* **1982**, *23*, 291-222.

0002-7863/83/1505-4489$01.50/0